Resonance Energy Transfer in the Solution Phase Photophysics of −Re(CO) 3 L + Pendants Bonded to Poly(4-vinylpyridine)

ARTICLE *in* THE JOURNAL OF PHYSICAL CHEMISTRY B · AUGUST 2008

Impact Factor: 3.3 · DOI: 10.1021/jp802241k · Source: PubMed

6 AUTHORS, INCLUDING:

Maria Juliarena
National University of Central Buenos Aires
20 PUBLICATIONS **118** CITATIONS
SEE PROFILE

Mario R. Feliz
National University of La Plata
69 PUBLICATIONS **695** CITATIONS
SEE PROFILE

G. Ferraudi
University of Notre Dame
186 PUBLICATIONS **2,512** CITATIONS
SEE PROFILE

Ezequiel Wolcan
National Scientific and Technical Research…
49 PUBLICATIONS **471** CITATIONS
SEE PROFILE

Resonance Energy Transfer in the Solution Phase Photophysics of $-Re(CO)_3L^+$ Pendants Bonded to Poly(4-vinylpyridine)

L. L. B. Bracco,[†,‡] M. P. Juliarena,[†,‡] G. T. Ruiz,[†,‡] M. R. Féliz,[§,‡] G. J. Ferraudi,[⊥] and E. Wolcan*[,†,‡]

INIFTA, Facultad de Ciencias Exactas, Universidad Nacional de La Plata, Casilla de Correo 16, Sucursal 4, (B1906ZAA) La Plata, Argentina, Notre Dame Radiation Laboratory, Notre Dame, Indiana 46556-0579

Received: March 14, 2008; Revised Manuscript Received: June 19, 2008

Polymers with general formula $\{[(vpy)_2vpyRe(CO)_3(tmphen)^+]\}_n\{[(vpy)_2vpyRe(CO)_3(NO_2\text{-phen})^+]\}_m$ (NO_2-phen = 5-nitro-1,10-phenanthroline; tmphen = 3,4,7,8-tetramethyl-1,10-phenanthroline); vpy = 4-vinylpyridine) were prepared and their morphologies were studied by transmission electron microscopy (TEM). Multiple morphologies of aggregates from these Re^I polymers were obtained by using different solvents. Energy transfer between $MLCT_{Re\rightarrow tmphen}$ and $MLCT_{Re\rightarrow NO_2\text{-phen}}$ excited states inside the polymers was evidenced by steady state and time-resolved spectroscopy. Current Förster resonance energy transfer theory was successfully applied to energy transfer processes in these polymers.

Introduction

Numerous studies have been concerned with thermal and photochemical reactions of inorganic polymers in the solid-state and solution phase. Interest in their photochemical and photophysical properties is driven by their potential applications in catalysis and optical devices.[1–12] The properties in the solution phase of the polymers **I** and **II** (see Scheme 1) were investigated in previous works.[1,9,12]

Marked differences were found between the photochemical and photophysical properties of polymers **I** and **II** and those of the related monomeric complexes, $pyRe^I(CO)_3L^+$ (L = phen, 2,2′-bpy). The main cause of these differences is the photogeneration of MLCT excited sates in concentrations that are much larger when $-Re^I(CO)_3L^+$ chromophores are bound to poly-4-vinylpyridine, $(vpy)_{600}$. This is the photophysical result of Re^I chromophores being crowded in strands of a polymer instead of being homogeneously distributed through solutions of a $pyRe^I(CO)_3L^+$ complex. The recently communicated association of several hundred strands of **II** in nearly spherical aggregates also contributes to the crowding of chromophores in small spaces in the solution, where the interaction between excited states becomes appreciable.[12]

The photogeneration of MLCT excited states in close vicinity within a polymer strand makes possible the study of energy transfer processes if donor and acceptor pendants are distributed along the strand.

Resonance energy transfer (RET) is a widely prevalent photophysical process through which an electronically excited "donor" molecule transfers its excitation energy to an "acceptor" molecule such that the excited-state lifetime of the donor decreases. If the donor happens to be a fluorescent molecule, RET is referred to as fluorescence resonance energy transfer, FRET. The importance of FRET is ubiquitous. In polymer science, Förster[13] theory is used to study the interface thickness in polymer blends, phase separation and conformational dynamics of polymers.[14–17] In biological sciences, the technique of FRET is being exploited to design supramolecular systems that can be used to harvest light in artificial photosynthesis as these light-harvesting systems of plants and bacteria involve unidirectional transfer of absorbed radiation energy to the reaction center via a multistep FRET mechanism. Recent advances in fluorescence resonance energy transfer have led to qualitative and quantitative improvements in the technique, including increased spatial resolution, distance range, and sensitivity. These advances, due largely to new fluorescent dyes, but also to new optical methods and instrumentation, have opened up new biological applications.[18] Besides these, FRET is commonly used in scintillators and chemical sensors.[19–23] We have applied ligand substitution reactions of the Re^I complexes to the derivatization of polymers **III**, **IV**, **V**, **VI**, and **VII** (Schemes 2 and 3). Polymers **III**−**VII** consist of a poly-4-vinilpyridine backbone with pendant chromophores $-Re^I(CO)_3(NO_2\text{-phen})$ and $-Re^I(CO)_3$(tmphen), where NO_2-phen and tmphen stand for 5-nitro-1,10-phenanthroline and 3,4,7,8-tetramethyl-1,10-phenanthroline, respectively. Morphologies of these polymers were studied using TEM. In polymers **V**−**VII**, we observed intramolecular RET between the luminescent $MLCT_{Re\rightarrow tmphen}$ excited states of $-Re^I(CO)_3$(tmphen) chromophores and the $MLCT_{Re\rightarrow NO_2\text{-phen}}$ excited states of $-Re^I(CO)_3$ (NO_2-phen). In this paper, luminescence quantum yields and lifetimes of polymers **V**−**VII** are discussed in terms of the current RET theories applicable to energy transfer between acceptors and donors randomly distributed in a polymer.

Experimental Part

Flash-Photochemical Procedures. Optical density changes occurring on a time scale longer than 10 ns were investigated with a flash photolysis apparatus described elsewhere.[24–26] In these experiments, 25 ns flashes of 351 nm (ca. 25−30 mJ/pulse) light were generated with a Lambda Physik SLL-200 excimer laser. The energy of the laser flash was attenuated to values equal to or less than 20 mJ/pulse by absorbing some of

* To whom correspondence should be adressed. Telephone: 54-221 425 7430/425 7291. Fax: +54 221 425 4642. E-mail: ewolcan@inifta.unlp.edu.ar.
† Member of CONICET staff.
‡ INIFTA, Facultad de Ciencias Exactas, Universidad Nacional de La Plata.
§ Member of CICPBA staff.
⊥ Notre Dame Radiation Laboratory.

10.1021/jp802241k CCC: $40.75
Published on Web 08/20/2008

SCHEME 1

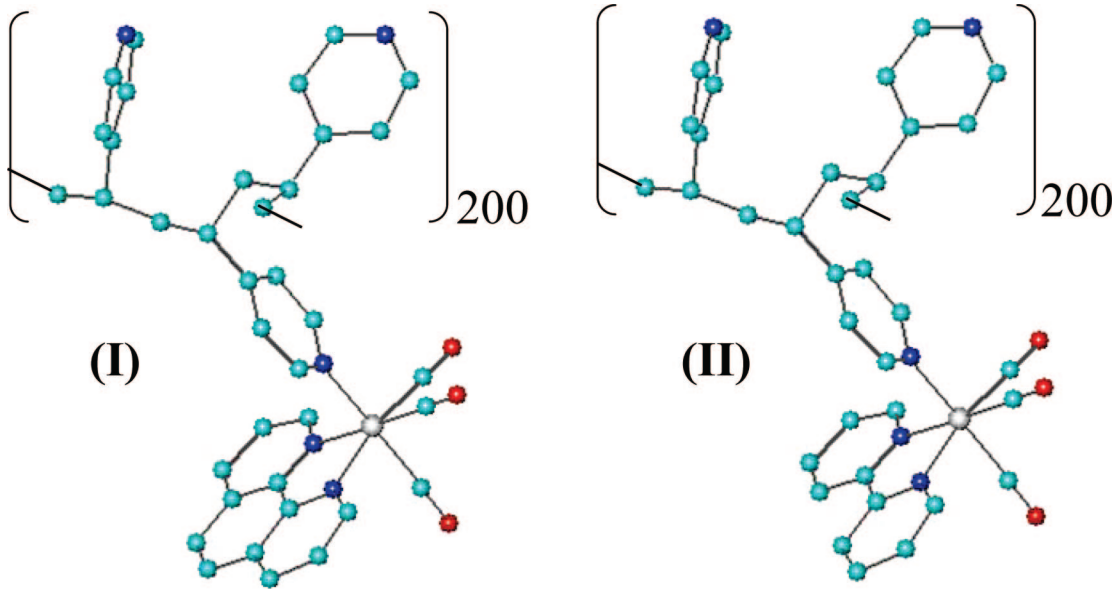

SCHEME 2

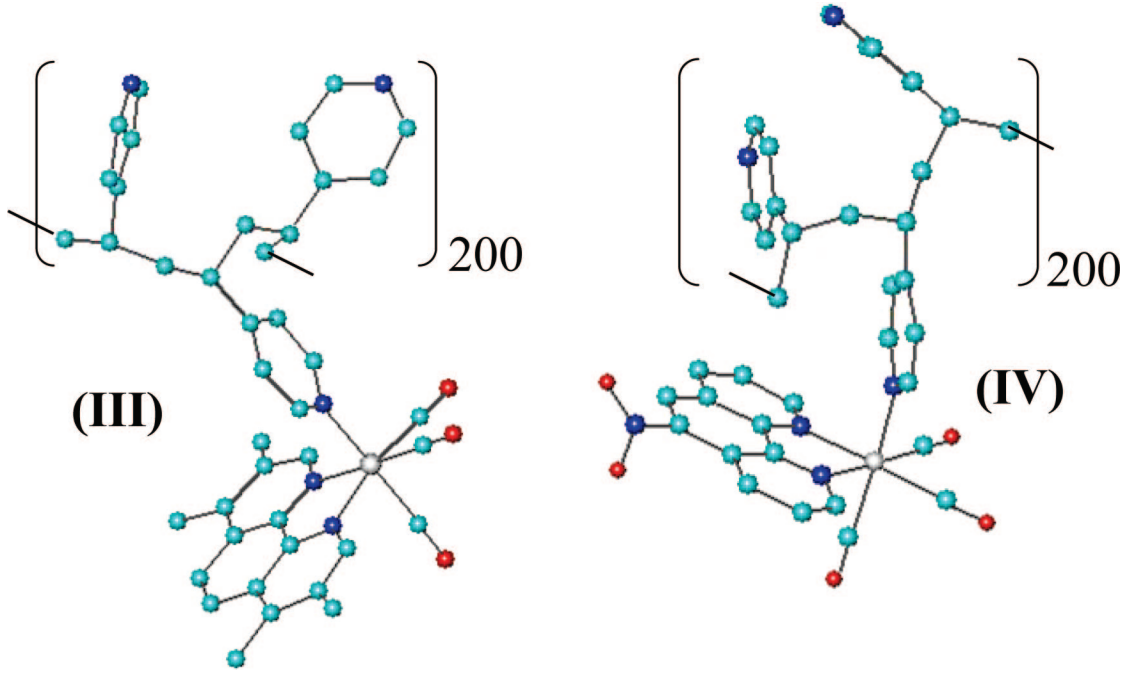

the laser light by solutions of $Ni(ClO_4)_2$ with appropriate optical transmittances.

$T = I_t/I_0$, where I_0 and I_t are, respectively the intensities of the light arriving to and transmitted from the photolysis cell. The transmittance, $T = 10^{-A}$, was routinely calculated by using the spectrophotometrically measured absorbance, A, of the solution. A right angle configuration was used for the pump and the probe beams. Concentrations of the complexes were adjusted to provide homogeneous profiles of photogenerated intermediates over the optical path, $l = 1$ cm, of the probe beam. To satisfy this optical condition, solutions were prepared with an absorbance equal to or less than 0.4 over the 0.2 cm optical path of the pump. All solutions used in the photochemical work were deaerated with streams of ultrahigh-purity N_2 before and during the irradiations.

A CPA-2010 1 kHz amplified Ti:sapphire laser system from Clark MXR and software from Ultrafast Systems were used for the observation of transient absorption spectra and the study of reaction kinetics in a femtosecond to 1.6 ns time domain. The flash photolysis apparatus provides 775, 387, or 258 nm laser pulses for excitation with a pulse width of 150 fs. Data points can be collected at intervals equal to or longer than 10 fs. A slow but constant flow of the solutions through a 2 mm cuvette was maintained during the photochemical experiments.

Time-resolved fluorescence experiments were carried out with a PTI flash fluorescence instrument. The excitation light was provided by a N_2 laser ($\lambda_{em} = 337$ nm, ca. 2 mJ/pulse and 200 ps bandwidth at half-height). All the solutions used in the photochemical work were deaerated for 1/2 h with streams of ultrahigh-purity N_2 before and during the irradiations. The fitting of data to analytical functions was made with commercially available routines, i.e. MicroCal Origin 7. The routines for the fittings used a nonlinear least-squares

SCHEME 3

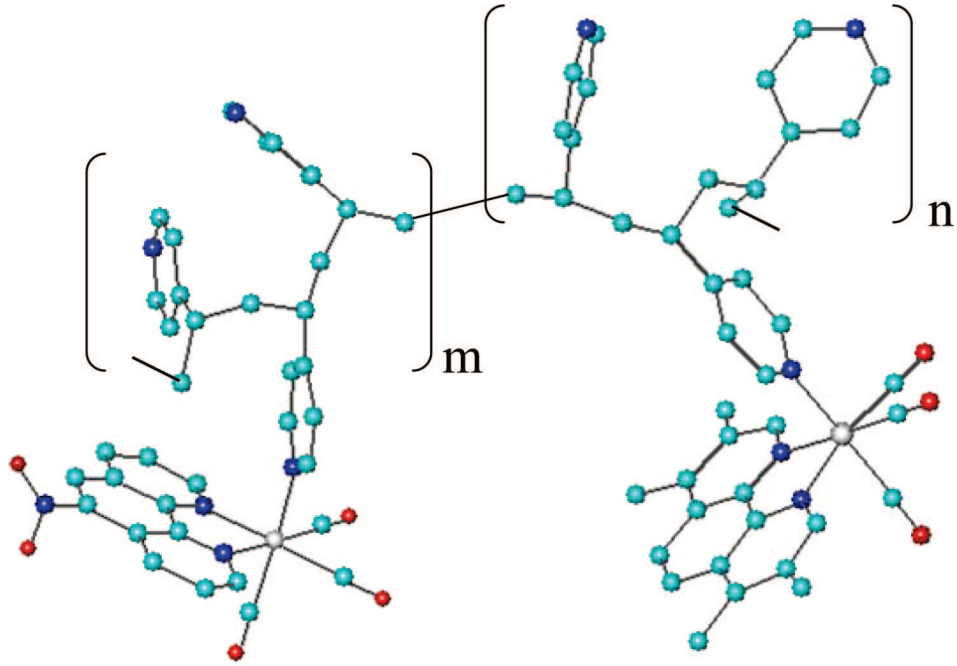

(V): n=180 ; m=20
(VI): n=150 ; m=50
(VII): n=100 ;m=100

method, and the goodness of the fits was established by the χ^2, standard, and quadratic deviations.

Steady State Irradiations. Emission spectra were obtained with a computer-interfaced Perkin-Elmer LS 50B spectrofluorimeter. Spectra were corrected for differences in spectral response and light scattering. Solutions were deaerated with O_2-free nitrogen in a gastight apparatus before recording the spectra. Emission quantum yields were measured relative to Rhodamine B in ethanol. Quantum yields were calculated according to eq. 1:

$$\phi_{em,sample} = \left(\frac{A_{ref}}{A_{sample}}\right)\left(\frac{I_{sample}}{I_{ref}}\right)\left(\frac{n_{sample}}{n_{ref}}\right)^2 \phi_{em,ref} \qquad (1)$$

where I is the integral of the emission spectrum and A is the absorbance of the sample or the reference at the excitation wavelength, and n is the solvent refraction index.

TEM. Transmission electron micrographs were recorded on a JEOL 100 CX electron microscope at an electron acceleration voltage of 80 kV with a nominal point-to-point resolution of 3 Å. The photos were taken at an amplification of 20000×.

Viscosity Measurements. The viscosity of a solvent mixture (glycerol/ethanol/dichloromethane, 5:3:2 v:v:v) at 25 °C was measured using a viscosimeter model Rotovisco HAAKE RV2 with a MK50 measuring head and a NV sensor system.

Materials. Reagent grade 5-nitro-1,10-phenanthroline (NO_2-phen) and 3,4,7,8-tetramethyl-1,10-phenanthroline (tmphen) were purchased from Aldrich and used as received. $CF_3SO_3Re(CO)_3(NO_2\text{-phen})$ and $CF_3SO_3Re(CO)_3$(tmphen) were prepared and purified by a literature procedure[1] that involves the reaction of $BrRe(CO)_3(NO_2\text{-phen})$ or $BrRe(CO)_3$(tmphen) with $AgCF_3SO_3$. Aldrich's poly-4-vinylpyridine, $(vpy)_{600}$, with M_w = ca. 6×10^4, was used without purification in the following preparations.

Preparation of $\{[(vpy)_2vpyRe(CO)_3(tmphen)^+]\}_{n\sim200}$ (III). The reaction of $CF_3SO_3Re(CO)_3$(tmphen) with $(vpy)_{600}$, with M_w = ca. 6×10^4,was used in the preparation of **III**. In the synthesis of the derivatized polymer, a solution that contained 40 mg of $CF_3SO_3Re(CO)_3$(tmphen) in 50 mL of CH_2Cl_2 (1.38×10^{-4} mol) was slowly added by being stirred into a solution containing 33.3 mg of $(vpy)_{600}$ (5.29×10^{-7} mol) in 25 mL of CH_2Cl_2. The amounts of $CF_3SO_3Re(CO)_3$(tmphen) and $(vpy)_{600}$ were chosen to have ~200 $-Re(CO)_3$(tmphen) groups per ~600 py present in the $(vpy)_{600}$ polymer. The solution was refluxed overnight. The mixture was rotatory evaporated to dryness, and the resulting solid was recrystallized by the slow addition of ethyl ether from CH_3CN. The resulting yellow complex was dried under vacuum at room temperature until a constant weight was obtained. Yield: 90% (87 mg). Anal. Calcd for **III**: H, 3.80; C, 50.26; N, 7.12. Found H, 3.82; C, 50.21; N, 6.82. FTIR (in KBr pellets). ν(CO)/cm^{-1}: 2029 (s) 1902 (br). UV−visible (CH_3CN): 248, 282, 325 (sh), 369 nm.

Preparation of $\{[(vpy)_2vpyRe(CO)_3(NO_2\text{-phen})^+]\}_{n\sim200}$ (IV). The reaction of $CF_3SO_3Re(CO)_3(NO_2\text{-phen})$ with $(vpy)_{600}$, with M_w = ca. 6×10^4, was used in the preparation of **IV**. In the synthesis of the derivatized polymer, a solution that contained 40 mg of $CF_3SO_3Re(CO)_3(NO_2\text{-phen})$ in 50 mL of CH_2Cl_2 (1.38×10^{-4} mol) was slowly added by being stirred into a solution containing 33.3 mg of $(vpy)_{600}$ (5.29×10^{-7} mol) in 25 mL of CH_2Cl_2. The amounts of $CF_3SO_3Re(CO)_3(NO_2\text{-phen})$ and $(vpy)_{600}$ were chosen to have ~200 $-Re(CO)_3(NO_2\text{-phen})$ groups per ~600 py present in the $(vpy)_{600}$ polymer. The solution was refluxed overnight. The mixture was rotatory evaporated to dryness, and the resulting solid was recrystallized by the slow addition of ethyl ether from CH_3CN. The resulting yellow complex was dried under vacuum at room temperature until a constant weight was obtained. Yield: 90% (87 mg). Anal.

Calcd for **IV**: H, 2.88; C, 45.76; N, 8.68. Found H, 3.35; C, 46.02; N, 8.48. FTIR (in KBr pellets). ν(CO)/cm^{-1}: 2034 (s), 1912 (br). UV−visible (CH_3CN): 267, 324, 359, 389 (sh) nm.

Preparation of the Polymers $\{[(vpy)_2vpyRe(CO)_3(tmphen)^+]\}_{n\sim180}\{[(vpy)_2vpyRe(CO)_3(NO_2\text{-}phen)^+]\}_{m\sim20}$ (V)-$\{[(vpy)_2vpyRe(CO)_3(tmphen)^+]\}_{n\sim150}\{[(vpy)_2vpyRe(CO)_3(NO_2\text{-}phen)^+]\}_{m\sim50}$ (VI) and $\{[(vpy)_2vpyRe(CO)_3(tmephen)^+]\}_{n\sim100}$-$\{[(vpy)_2\text{-}vpyRe(CO)_3(NO_2\text{-}phen)^+]\}_{m\sim100}$ (VII). Polymers with general formula $\{[(vpy)_2vpyRe(CO)_3(tmphen)^+]\}_n\{[(vpy)_2vpyRe(CO)_3(NO_2\text{-}phen)^+]\}_m$—where **V** stands for $n = 180$ and $m = 20$, **VI** stands for $n = 150$ and $m = 50$, and **VII** stands for $n = 100$ and $m = 100$—were prepared by a reaction of the appropriate $CF_3SO_3Re(CO)_3$(tmphen) and $CF_3SO_3Re(CO)_3(NO_2$-phen) molar mixtures with $(vpy)_{600}$ in the same way as polymers **III** and **IV**. In polymers $\{[(vpy)_2vpyRe(CO)_3(tmphen)^+]\}_n\{[(vpy)_2vpyRe(CO)_3(NO_2\text{-}phen)^+]\}_m$, a ratio of 200 - $Re(CO)_3(L)$ groups per 600 py present in the $(vpy)_{600}$ polymer was maintained. However, the ratio $m/(m + n)$ was varied from 10% (in polymer **V**) to 25% (in polymer **VI**) and 50% (in polymer **VII**). Anal. Calcd for **V**: H, 3.70; C, 49.81; N, 7.27. Found: H, 4.49; C, 49.5; N, 6.15. FTIR (in KBr pellets). ν(CO)/cm^{-1}: 2029 (s) 1902 (br). UV−visible (CH_3CN): 248, 282, 325, 369 nm. Anal. Calcd for **VI**: H, 3.57; C, 49.14; N, 7.50. Found: H, 3.85; C, 49.35; N, 7.09. FTIR (in KBr pellets). ν(CO)/cm^{-1}: 2030 (s) 1906 (br). UV−visible (CH_3CN): 249, 282, 325, 369 nm.

Anal. Calcd for **VII**: H, 3.34; C, 48.01; N, 7.90. Found: H, 3.49; C, 47.86; N, 7.91. FTIR (in KBr pellets). ν(CO)/cm^{-1}: 2032 (s) 1907 (br). UV−visible (CH_3CN): 252, 266 (sh), 274 (sh), 326, 350, 373 nm.

As can be observed from these figures, there is a systematic shift of ν(CO) to higher wavenumbers when the content of $Re(CO)_3(NO_2\text{-}phen)^+$ groups is increased relative to the number of $Re(CO)_3(tmphen)^+$ pendants from polymer **V**−**VII**. Moreover, in the region between 1300 and 1350 cm^{-1}, where the ligand tmphen has no significant absorptions, the ligand NO_2-phen has a characteristic absorption band centered at 1130 cm^{-1}. In the polymers **V**−**VII**, an increase of the absorption peak at 1330 cm^{-1} was observed in agreement with the increasing amounts of $Re(CO)_3(NO_2\text{-}phen)^+$ pendants relative to $Re(CO)_3(tmphen)^+$ pendants when passing from **V** to **VII**.

Results

Solvent-Cast Films of the Polymers. The morphologies of the polymers **III**−**VII** were studied by transmission electron microscopy (TEM). When taking photos, the polymer films were not stained with any chemicals, and the contrast of the image in the TEM photos can only originate from the rhenium complexes incorporated to the polymers. Multiple morphologies of aggregates from these Re^I polymers were obtained by using different solvents. TEM images of acetonitrile and dichloromethane-cast films of the polymers are shown in Figure 1 and Figure 2, respectively.

Steady State Photophysics. Deaerated solutions of the polymers **III**−**VII** with total concentration of the Re^I chromophores equal to or less than 1×10^{-4} M in CH_3CN were irradiated at 380 nm to record the emission spectrum. The emission spectrum of polymer **III** in deoxygenated CH_3CN at room temperature exhibited an unstructured band centered at 520 nm. Polymer **IV** is nonluminescent. Polymers **V**−**VII** have luminescence spectra, which are the same in shape to that of polymer **III**. The luminescence quantum yield (ϕ_{em}) of polymer **III** is around 0.03. Polymer **V** has a ϕ_{em} that is nearly $^1/_3$ lower than that of polymer **III**. ϕ_{em} decreases monotonically from polymer **V** to polymer **VII**. Table 1 summarizes all the measured ϕ_{em}. It shows also the ϕ_{em} measured with molar mixtures of polymers **III** and **IV**, i.e., to obtain the same $m/(n + m)$ in the mixture as there is in polymers **V**−**VII**. ϕ_{em} determined for the mixtures 90% **III** + 10% **IV**, 75% **III** + 25% **IV**, and 50% **III** + 50% **IV** are noticeably higher than those of polymers **V**, **VI**, and **VII**, respectively. For instance, while ϕ_{em} of the mixture 50% **III** + 50% **IV** is nearly $^1/_2$ ϕ_{em} of polymer **III**, ϕ_{em} of polymer **VII** is nearly 2 orders of magnitude lower than that of polymer **III**.

Quenching Experiments. The quenching of the luminescence of the Re^I polymer **III** by $ClRe(CO)_3(NO_2$-phen) was studied using steady state techniques under similar experimental conditions ([Re^I] in the polymer $\sim 1 \times 10^{-4}$ M) to those utilized in quantum yield measurements in a solvent mixture (glycerol/ethanol/dichloromethane, 5:3:2 v:v:v, hereafter referred as GED) with a viscosity of $\eta = 0.23$ poise varying [$ClRe(CO)_3(NO_2$-phen)] between 1×10^{-4} and 1×10^{-3} M. The quenching followed a Stern−Volmer kinetics with a $K_{sv} = 3.1 \times 10^3$ M^{-1}. In acetonitrile, the quenching also followed a Stern−Volmer kinetics with a $K_{sv} = 1.9 \times 10^4$ M^{-1}. See Figure 3.

Time-Resolved Absorption Spectroscopy of Polymers III, V, VI, and VII. Transient absorption spectra in the 15 ns to microsecond time domain were recorded with a 351 nm excimer laser flash photolysis setup. This excitation wavelength produces optical excitation of the MLCT absorption bands of the polymers. When N_2-deaerated acetonitrile solutions of the polymers **III**, **V**, **VI** and **VII** were irradiated at 351 nm, the transient spectra observed after the 10 ns irradiation decayed biexponentially over a period of several microseconds. The oscillographic traces were fitted to two exponentials with lifetimes τ_{fast} and $\tau_{slow.}$ The lifetimes τ_{fast} and τ_{slow} are collected in Table 1. Transient spectra recorded with either polymer at times immediately after the laser pulse decay, i.e., 20 ns (showing $\Delta A_{t=0}$ values vs wavelength), showed the spectra of the $^3MLCT_{Re\rightarrow tmphen}$ excited states decaying by radiative and nonradiative processes. The transient spectra generated when these polymers were irradiated at 351nm under the same photochemical conditions (i.e., [Re^I] and laser energy/pulse) are shown in Figure 4. It can be observed that transients generated after 351 nm excitation of polymers **III**, **V**, **VI**, and **VII** have the same spectral features albeit the initial amount (proportional to $\Delta A_{t=0}$) decreases from **III** to **VII**. Luminescence lifetimes of polymers **III**, **V**, **VI**, and **VII** were measured in their CH_3CN deoxygenated solutions using a PTI flashfluorescence equipment with $\lambda_{exc} = 337$ nm. The decay of the luminescent profiles for polymer **III** were monoexponential with a lifetime of $\tau_{em} = 5.12$ μs. However, the decay of the luminescent profiles for polymers **V**−**VII** were nonexponential and were fitted following a modification of the Förster treatment,[21,27] eq 2.

$$N_t = N_0 \exp\left[-\frac{t}{\tau_D} - a\sqrt{t/\tau_D}\right] \qquad (2)$$

Time-Resolved Absorption Spectroscopy of polymer IV. Transient absorption spectra in the femtosecond to nanosecond time domain were recorded with a Ti:sapphire laser flash photolysis instrument providing 387 nm laser pulses for the irradiation of the polymer. The femtosecond to nanosecond transient spectra of the excited states produced ~4 ps after the 387 nm flash irradiation of 1.5×10^{-6} M of polymer **IV** (i.e., [Re^I] = 3×10^{-4}M) are shown in Figure 5. The transient spectrum consists of three absorption bands, two with maxima at 450 and 600 nm, respectively, and a third one with $\lambda_{max} >$ 750 nm. It decays monoexponentially over a period of 1600 ps with a lifetime of 230 ps.

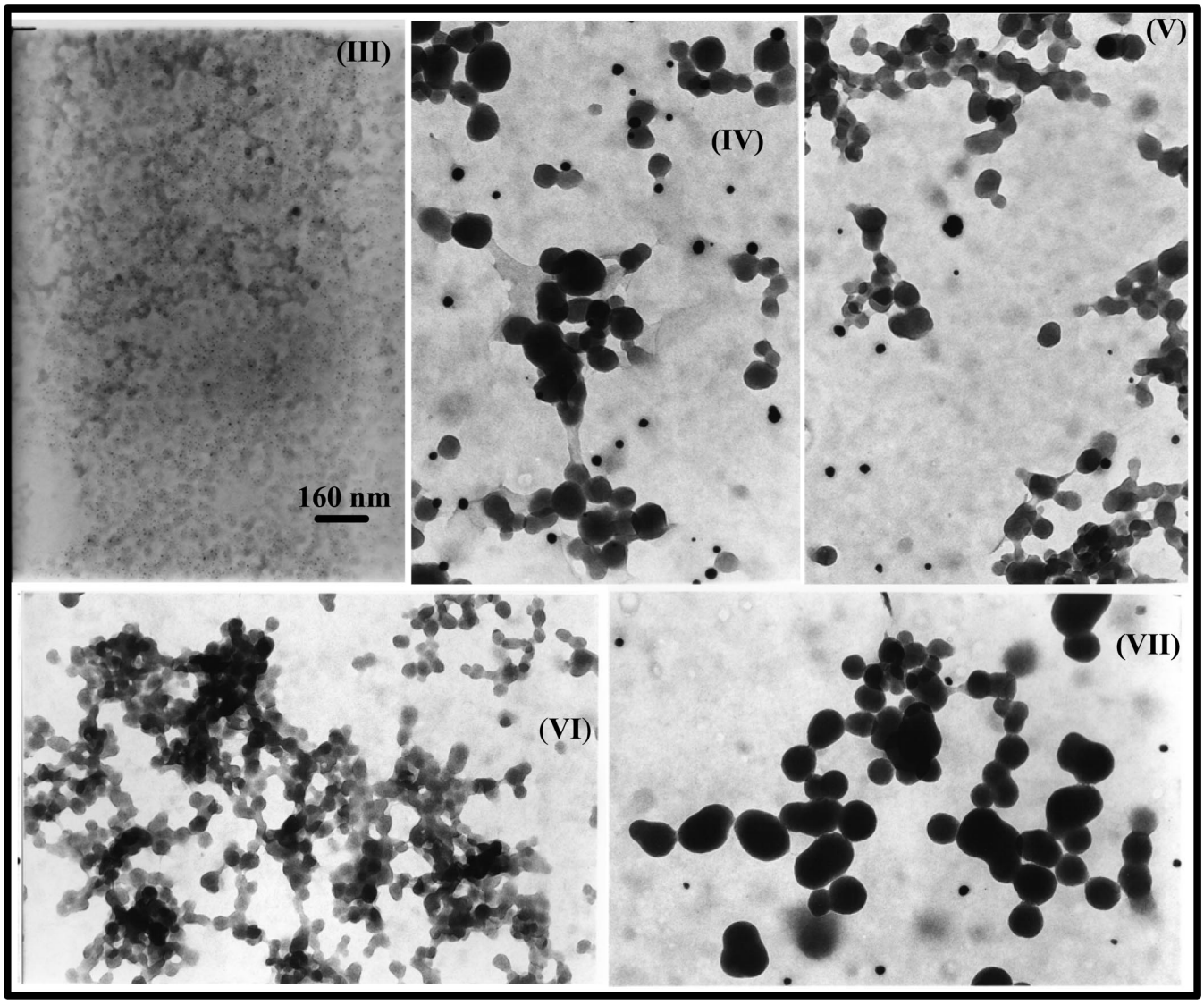

Figure 1. Acetonitrile-cast films of polymers **III**, **IV**, **V**, **VI**, and **VII**. The same scale bar applies to all the films in the figure.

Discussion

Morphologies of the Polymers. Morphologies of the polymers differed when the cast films were obtained either from acetonitrile or dichloromethane solutions. When the solvent was acetonitrile, Figure 1, in the solid phase of polymer **IV**, the Re^{I} complexes aggregate and form isolated nanodomains that are dispersed in the $(vpy)_{600}$ backbone. The dimensions of the aggregates are between 80 and 160 nm and are mainly spherical in shape. However, polymer **III** does not aggregate to form large nanodomains and only small spherical objects with diameter between 5 and 30 nm, are observed. In polymers **V**−**VII**, TEM images suggest the formation of aggregates of increasing size from **V** to **VII**. It should be noted that the dimensions of the nanodomains are considerably larger than the full stretch length of the polymers. As a result, it is likely that they contain more than one layer of polymers. The situation is completely different in dichloromethane. Figure 2 shows TEM images of dichloromethane-cast films of polymers **III**−**VII**. Vesicles were obtained for polymers **III**, **V**, and **VI**. The vesicular nature is evidenced by a higher transmission in the center of the aggregates than around their periphery in the TEM pictures. The sizes of the vesicles are very polydisperse with outer diameters ranging from 140 nm to large compound vesicles with diameters up to 1.4 μm. More interestingly, polymer **IV** formed branched tubular structures intertwined in a net. The morphologies shown for polymer **VII** are the intermediate shape of vesicles and tubules. It is interesting to note that micellar-like aggregates have been previously observed from TEM images of acetonitrile-cast films of polymer **II** and polymers $\{(vpy-[Re(CO)_3(2,2'\text{-bpy})])_m(vpy\text{-}[Re(CO)_3(phen)])_n(vpy)_p\}-(CF_3SO_3)_{m+n}\}$, (vpy = 4-vinylpyridine).[12,28] We can rationalize the solvent effect upon aggregation of $Re^{I}-(vpy)_{600}$ polymers as follows. For instance, $(vpy)_{600}$ is nearly insoluble in acetonitrile, but this solvent is a good one for the $Re^{I}-(vpy)_{600}$ polymers. Then, it is plausible to imagine that the inner core of the micelles present in acetonitrile will be formed mainly by the free pyridines of the $Re^{I}-(vpy)_{600}$ polymers and the outer part will be constituted mainly by the solvated Re^{I} pendants. The situation is reversed in dichloromethane as this solvent is a good one for $(vpy)_{600}$. Moreover, polymers **I** and **II** cannot be dissolved in that solvent while solubility of polymers **III**−**VII** is considerably lower in dichloromethane than in acetonitrile. In vesicles, however, a pool of dichloromethane molecules are solvating the uncoordinated pyridines of the polymer in the inner and outer region of the vesicle while the Re^{I} pendants mainly remain inside the membrane of the vesicle.

Photophysical Properties. ***Steady State Luminescence.*** The photophysical properties of polymers **III** and **IV** are quite

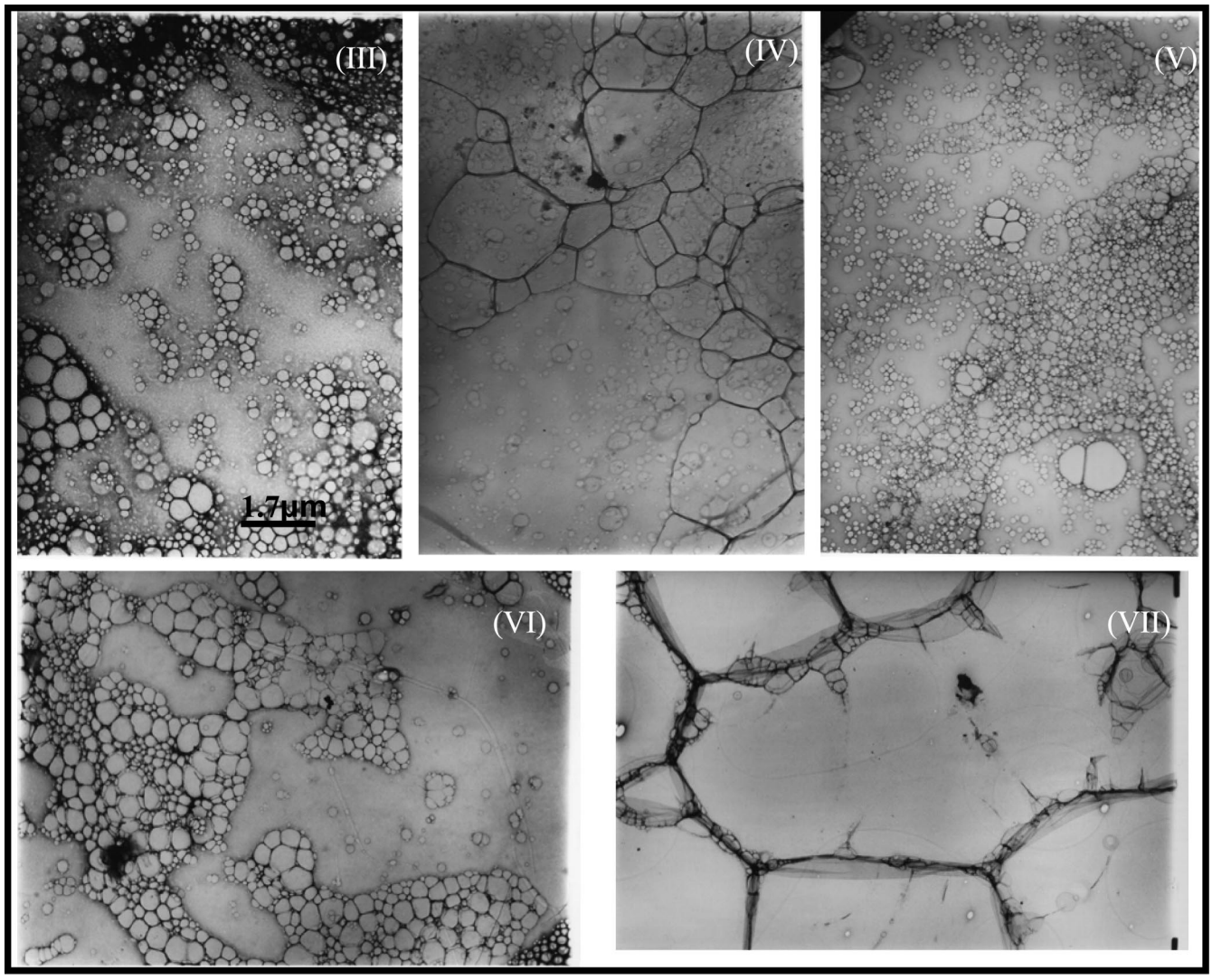

Figure 2. Dichloromethane-cast films of polymers **III**, **IV**, **V**, **VI**, and **VII**. The same scale bar applies to all the films in the figure.

TABLE 1: Photophysical Properties of Polymers III, IV, V, VI, and VII in Acetonitrile at Room Temperature

	ϕ_D[a,b]	τ_{fast}, ns[c]	τ_{slow}, μs[c]	energy transfer efficiency $E_T^j = 1 - \phi_D^j/\phi_{mb}^j$
		Polymers		
III	0.035	$(7.4 \pm 0.9) \times 10^2$	3.4 ± 0.5	
IV	$<10^{-4}$	0.23 ± 0.01[d]		
V	0.013	$(1.1 \pm 0.2) \times 10^2$	1.13 ± 0.07	0.58
VI	0.0038	50 ± 10	0.59 ± 0.07	0.85
VIII	0.0007	<10	0.047 ± 0.006	0.94
Molar Blends				
90% **III** + 10% **IV**	0.031			
75% **III** + 25% **IV**	0.026			
50% **III** + 50% **IV**	0.0125			

[a] Emission quantum yields of polymers **III**, **IV**, **V**, **VI**, and **VII**. Error ± 10%. [b] Emission quantum yields, ϕ_D, measured with molar blends of polymers **III** and **IV** in order to obtain the same $m/(n + m)$ in the blend as there is in polymers **V**−**VII**. Error ± 10%. See text for details. [c] Obtained from a curve fit analysis with two exponentials from transient absorbance decays in flash photolysis experiements (λ_{ex} = 351 nm). [d] Obtained from a monoexponential decay of the transient absorbance in femtosecond laser photolysis experiments (λ_{ex} = 387 nm).

different. Polymer **III** has a luminescence quantum yield of $\phi_{em} \sim 0.03$ and a luminescence lifetime of ~5 μs, a value that is between $^1/_2$ and $^1/_3$ of that of the corresponding monomer.[29] Though a longer lifetime for the monomer than for the polymer could be associated with the availability of new deactivation pathways for the MLCT in the polymer due to vibration modes present in the poly(vinylpyridine) backbone.[9]

On the other hand, polymer **IV** is nonluminescent ($\phi_{em} < 1 \times 10^{-4}$). Moreover, after excitation of a polymer **IV** solution in CH_3CN with λ_{exc} = 387 nm, the transient generated decayed very fast with a lifetime of 230 ps. Taking into account the spectral similarities between the spectrum of the $MLCT_{Re\rightarrow NO_2\text{-phen}}$ in the monomers $LRe(CO)_3(NO_2\text{-phen})^{+}$[30] with that of Figure 5, the transient generated in the femtosecond to nanosecond time domain of polymer **IV** can be assigned to the $^3MLCT_{Re\rightarrow NO_2\text{-phen}}$ excited-state of $Re(CO)_3(NO_2\text{-phen})^+$ pendants in the polymer decaying nonradiatively. Moreover, the $^3MLCT_{Re\rightarrow NO_2\text{-phen}}$ excited states are very

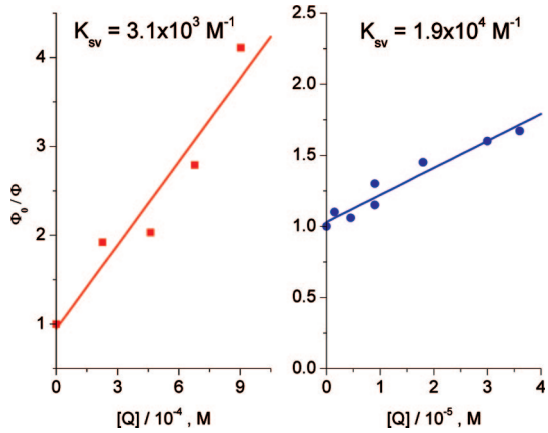

Figure 3. Stern−Volmer plots for the quenching of the luminescence of the Re^{I} polymer **III** by $ClRe(CO)_3(NO_2\text{-phen})$ in acetonitrile (●) and in GED (■). See text for details.

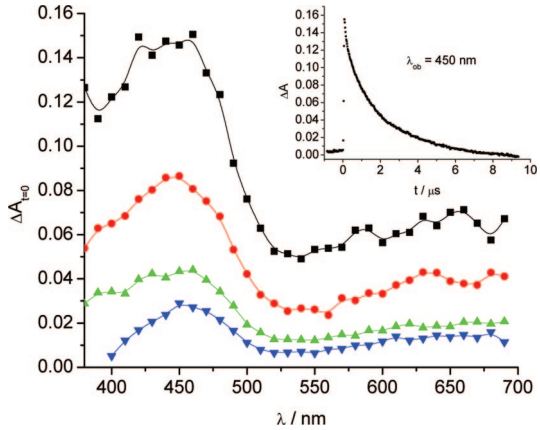

Figure 4. Difference absorption spectrum of the ^{3}MLCT excited states of the -$Re(CO)_3(tmphen)^+$ pendants in polymers **III** (■), **V** (●), **VI** (▲), and **VII** (▼). Transient spectra recorded with either polymer at times immediately after the laser pulse decay showing $\Delta A_{t=0}$ vs λ. The solutions of the polymers in CH_3CN contained a concentration of Re^{I} chromophores of $[Re^{I}] = 5.0 \times 10^{-4}$ M, and it was flash irradiated at 351 nm. The inset is a typical oscillographic trace revealing the biexponential decay of the absorbance at $\lambda_{ob} = 450$ nm.

short-lived: 7.6, 170, and 43 ps for $L = Cl^-$, 4-Etpy, and imH, respectively, in CH_3CN solutions.[30] In this regard, the lifetime of the $MLCT_{Re\rightarrow NO2\text{-}phen}$ in the complex with L= 4-Etpy is very similar to that of polymer **IV**.

From the comparison of ϕ_{em} values for polymers **V**, **VI**, and **VII** with the corresponding ϕ_{em} of the molar blends 90% **III** + 10% **IV**, 75% **III** + 25% **IV** and 50% **III** + 50% **IV**, it can be inferred that the substitution of pendants $Re(CO)_3(tmphen)^+$ by pendants $Re(CO)_3(NO_2\text{-phen})^+$ in the poly-4-vinylpyridine backbone produces a decrease in ϕ_{em} that is in proportion to the number of $Re(CO)_3(NO_2\text{-phen})^+$ pendants relative to that of $Re(CO)_3(tmphen)^+$ pendants due to an energy transfer process that involves the excited states $MLCT_{Re\rightarrow tmphen}$ and $MLCT_{Re\rightarrow NO_2\text{-}phen}$. This energy transfer is justified from a thermochemical stand point because the UV−vis spectra of polymers **III** and **IV** show that $^1MLCT_{Re\rightarrow tmphen}$ is higher in energy than $^1MLCT_{Re\rightarrow NO_2\text{-}phen}$ excited state. This higher energy is not surprising because the NO_2− group, which is withdrawing electronic charge from the phen ligand makes the charge transfer from the Re^{I} to the NO_2-phen energetically more favored than that of Re^{I} to phen. The situation is reversed with the tmphen ligand as in the chromophore $Re(CO)_3(tmphen)^+$ the methyl groups

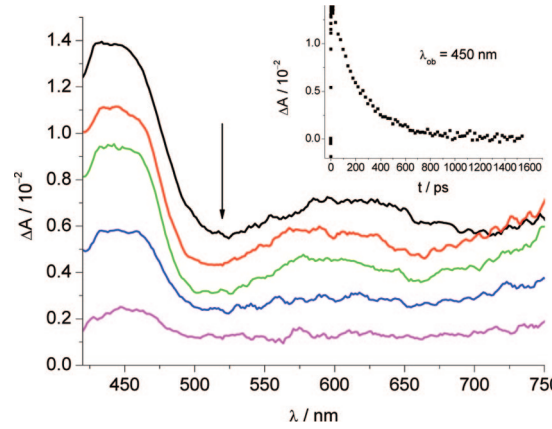

Figure 5. Time resolved absorption spectra recorded on a femtosecond to nanosecond time scale after the 387 nm flash irradiation of polymer **IV** solutions in CH_3CN. The spectra were recorded at 2, 60, 100, 200, and 400 ps time delays after the laser pulse. The solutions of the polymers in CH_3CN contained a concentration of Re^{I} chromophores of $[Re^{I}] = 3.0 \times 10^{-4}$ M. The spectra evolved in the direction of the arrow. The inset is a typical oscillographic trace revealing the monoexponential decay of the absorbance at $\lambda_{ob} = 450$ nm.

are injecting electronic charge to the substituted phen ligand and the charge transfer from the Re^{I} to tmphen is energetically less favored than that of Re^{I} to phen. On the other hand, there is no experimental evidence of a charge transfer in the quenching of the $^3MLCT_{Re\rightarrow tmphen}$ as no photoproducts and/or intermediates (i.e., the formation of $Re(CO)_3(tmphen)^{2+}$ and $Re(CO)_3(NO_2\text{-phen})^{\bullet}$ species) were observed after the decay of $^3MLCT_{Re\rightarrow tmphen}$ in flash photolysis experiments. The quenching of the $^3MLCT_{Re\rightarrow tmphen}$ by the $Re(CO)_3(NO_2\text{-phen})^+$ pendants must be an energy transfer process rather than an electron transfer one.

ϕ_{em} of the molar blends 90% **III** + 10% **IV**, 75% **III** + 25% **IV** and 50% **III** + 50% **IV** can be compared to the ϕ_{em} values that would have been expected for polymers **V**, **VI**, and **VII** if no energy transfer between $[Re(CO)_3(tmphen)^+]^*$ and $Re(CO)_3(NO_2\text{-phen})^+$ pendants had occurred, eqs 3 and 4

$$\phi_D = \left(\frac{A}{A_T}\right)\phi_D{}^0 \tag{3}$$

$$\frac{A}{A_T} = \frac{n\varepsilon_{\lambda,n}}{n\varepsilon_{\lambda,n} + m\varepsilon_{\lambda,m}} \tag{4}$$

where A is the absorbance of the donor $Re(CO)_3(tmphen)^+$ at wavelength λ, A_T is the total absorbance of the solution and $\varepsilon_{\lambda,n}$ and $\varepsilon_{\lambda,m}$ are the molar extinction coeffients of the donor $Re(CO)_3(tmphen)^+$ and the acceptor $Re(CO)_3(NO_2\text{-phen})^+$ at wavelength λ, respectively, and $\phi_D{}^0$ is the emission quantum yield of the donor, i.e. 0.0347 for polymer **III**. Given the values of 5.5×10^5 and 7.8×10^5 M^{-1} cm^{-1} for the extinction coefficients of polymers **III** and **IV** at 380 nm, ϕ_D values of 0.0298, 0.0236, and 0.0142 can be calculated for polymers **V**, **VI**, and **VII**, respectively. Those ϕ_D values are similar to the experimental values measured for the blends 90% **III** + 10% **IV**, 75% **III** + 25% **IV** and 50% **III** + 50% **IV**, which are 0.031, 0.026, and 0.0125, respectively (see Table 1). Therefore, it can be concluded that there is not bimolecular (i.e., intermolecular) quenching between excited $Re(CO)_3(tmphen)^+$chromophores in polymer **III** and acceptors $Re(CO)_3(NO_2\text{-phen})^+$ in polymer **IV** in the blends.

Triplet−triplet (T−T) RET is overall a spin-allowed process; spin is conserved between the initial state $^3(^3D^*\text{-}^1A)$ and the

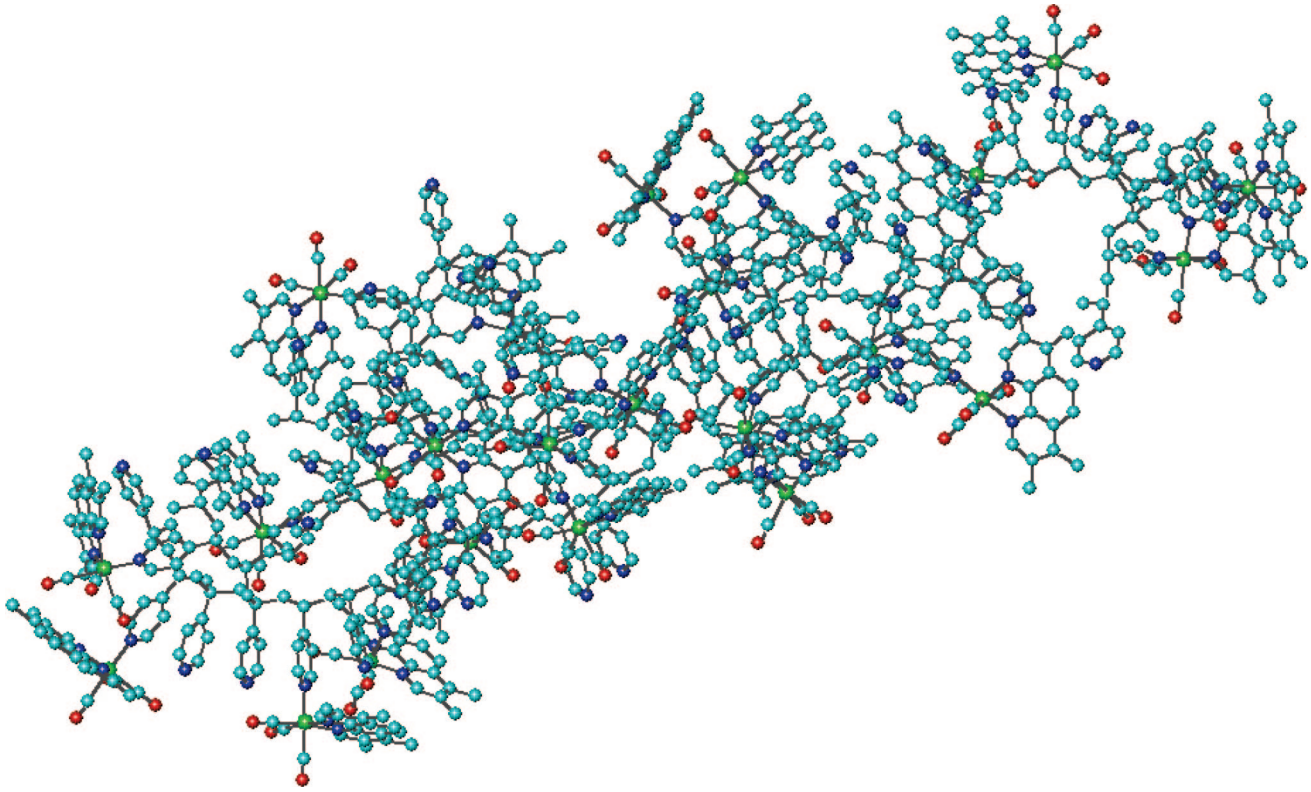

Figure 6. Side-on view of polymer $\{[(vpy)_2vpyRe(CO)_3(tmphen)^+]\}_{n\sim200}$ showing the distribution of Re^I centers (green balls) along the $(vpy)_{600}$ backbone. Other atoms: C (cyan balls), O (red balls), and N (blue balls).

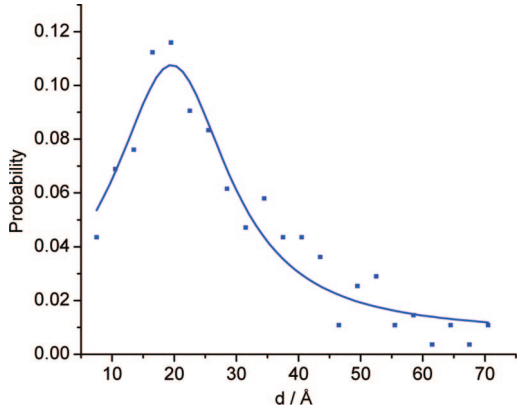

Figure 7. Distribution of distances between the Re^I centers in polymer $\{[(vpy)_2vpyRe(CO)_3(tmphen)^+]\}_{n\sim200}$.

final state $^3(^1D-^3A^*)$. It is known that T−T RET cannot be mediated by the Coulombic interaction because it is spin-forbidden. Therefore, spin selection rules for dipole−dipole transfer are that no change of spin for either donor or acceptor transitions can occur.[31] A Coulombic interaction can, in principle, promote T−T RET via spin−orbit coupling terms in the Hamiltonian. However, spin−orbit coupling-mediated Coulombic coupling would usually be much smaller than the normal Coulombic interaction between the singlet states of donor and acceptor.[31]

On the other hand, spin forbidden transitions in the donor have been observed leading to an enhanced lifetime and long-range transfer while no such compensation applies when the transition is spin forbidden in the acceptor.[32] FRET studies in organic polymers are usually discussed in terms of dipole−dipole interactions since D and A are pendants attached to the organic backbone, no diffusion and encounter complexes are likely to occur between them and Dexter's exchange[32] mechanism for energy transfer is disfavored against the dipole−dipole interaction. When the molecular species are transition metal complexes in fluid solutions and when metal centered ligand field (or d−d) excited states are involved, the basic principles for description of the energy transfer reaction coordinate are not altogether clear. Thus the much studied and well understood dipole−dipole, or Förster, mechanism for energy transfer is not strictly applicable when spin forbidden excited states are involved. However, FRET has also been employed in energy transfer studies involving inorganic systems where triplet (or higher spin multiplicity, as in the case of lanthanides) states may be involved in the energy transfer process.[16,18–22,33–40]

Polymers **V**, **VI**, and **VII** consist of donors $Re(CO)_3(tmphen)^+$ and acceptors $Re(CO)_3(NO_2\text{-phen})^+$ distributed at random through coordination to the pyridines of the $(vpy)_{600}$ polymer backbone. Locally, there should be regions with no pyridine spacer (D−A, D−D, A−A), a single pyridine spacer (D−py−A, D−py−D, A−py−A) and two or more spacers (D−py−py−A, D−py−py−D, A−py−py−A), etc. MLCT lifetimes and energy transfer dynamics are dependent on the local environment, and there is a distribution of sites on individual polymer strands. According to a molecular modeling calculation (see below) the average periphery-to-periphery distance between nearest neighbors might be about 7 Å in these polymers. Moreover, local segmental motions could decrease that distance to well below 7 Å. Therefore, at distances between nearest neighbors of 7 Å or lower, the detailed energy-transfer mechanism, whether Förster (Coulomb) or Dexter (exchange) or a combination of the two is unknown. Given its $1/R^6$ distance dependence, Förster transfer is favored over Dexter transfer at long distances since Dexter transfer varies exponentially with distance. As Förster transfer requires that spin be conserved separately at the energy transfer donor and acceptor, this

condition could be overcome if spin−orbit coupling is of importance, as for instance in Ru^{II} and Os^{II} polystyrene polymers.[41]

To elucidate further the nature of the energy transfer process in our polymeric systems, we performed a quenching experiment of polymer **III** luminescence using $ClRe(CO)_3(NO_2\text{-phen})$ as energy acceptor in a solvent mixture GED where diffusion was somewhat restricted. For that solvent, with a viscosity of η=0.23 poise, a diffusion rate constant $k_{diff} = 2.0 \times 10^8$ M^{-1} s^{-1} can be calculated.[42] This value of k_{diff} is similar to that of 1,2-ethanediol (η = 0.20 poise),[42] $k_{diff} = 3.0 \times 10^8$ M^{-1} s^{-1}. As in GED solvent system quenching is observed at $ClRe(CO)_3(NO_2\text{-phen})$ concentrations as low as 2×10^{-4} M, a diffusion lifetime $\tau_{diff} = 1/(k_{diff}[Q]) = 25$ μs can be calculated for that quencher concentration. This τ_{diff} is nearly 5 times longer than the luminescence lifetime of polymer **III**. At a quencher concentration $\sim 2 \times 10^{-4}$ M the mean distance between molecules is ∼110 Å.[42] Therefore, within the excited-state lifetime of the polymer, quencher molecules will be able to diffuse only ∼20−30 Å and on the average they will be far apart (distances >70 Å) from the luminescent center. At those large separation distances between D and A, Dexter's mechanism of energy transfer is disfavored against Förster's.

Time Resolved Luminescence. Luminescence decay profiles of polymers **V**, **VI**, and **VII** were fitted using eq 2 giving the values of a = 1.90, 4.6, and 19.3, respectively with $\tau_D = 5.12$ μs. Values of $N \approx 1.1$, 2.6, and 11 can be calculated[27] for polymers **V**−**VII** using the vales of a = 1.90, 4.6, and 19.3, respectively.

A calculation of R_F[27] for the present system gives a value of 10.7 Å. This value is in the lower limit of R_F values (typically between 10 and 70 Å) due to the poor overlap between the emission spectrum of the donor $^3MLCT_{Re\rightarrow tmphen}$ and the absorption spectrum of the acceptor $Re(CO)_3(NO_2\text{-phen})^+$. Using this value of R_F and the values of a obtained above from the luminescence decay fitting, values of $\rho = 2.1\text{x } 10^{-4}$, 5.05×10^{-4} and 2.1×10^{-3} $N_{acceptors}/Å^3$ can be calculated in polymers **V**, **VI**, and **VII**, respectively.[27]

In order to better appreciate effect of the structural and morphological characteristics of the polymer in the photophysical properties, the results of a molecular modeling calculation on polymer **III** are illustrated in Figure 6. The calculations were performed using the HYPERCHEM 7 program using the Molecular Mechanics Optimization with a Polak−Ribiere (conjugate gradient) algorithm based on an atactic polymer with a load of $Re(CO)_3(tmphen)^+$ pendants similar to that of polymer **III**. In the calculation, the constructed polymer contained 24 $Re(CO)_3(tmphen)^+$ pendants attached to $^1/_3$ of a total of 72 pyridines. It represents about a 12% of the full polymer **III** (where there are ∼200 $Re(CO)_3(tmphen)^+$ pendants attached to $^1/_3$ of the ∼600 pyridines present in the polymer). One side-on view of the polymer is illustrated. No solvent molecules were included in these calculations and they are only elaborate cartoons of the real molecules. They do, however, give insight into the polymer structure which can help to visualize the distribution of distances between the Re^I centers. As an example, the positive charges of the Re^I centers and the large volumes of the Re^I pendants force the polymer to adopt extended, rodlike structures. We constructed a distance-map (taking into account all the possible distances between the 24 Re^I centers in the polymer model) which is shown in Figure 7. This figure shows the probability of finding a Re^I pendant at a distance d(Re−Re) from a reference Re^I pendant vs d(Re−Re). The curve resembles a Gaussian that has been "truncated" at distances ∼7 Å (which means that it is physically impossible to have two Re^I pendants at a closer vicinity with a distance d(Re−Re) below that value). Close neighbors (d(Re−Re) ∼ 7 Å) contribute 4% to the total of the cases. The maximum of the distribution, which could be visualized as a mean Re−Re distance, occurs at ∼ 20 Å and contributes 12% of the total cases. Re−Re distances beyond 30 Å contribute with less than 4% of the total possible distances. The number of neighbors at distances around $R_F \sim 11$ Å is between 7 and 8% of the total. In polymers **V**, **VI**, and **VII**, the distribution of distances should be similar to that of polymer **III** as the pendants $Re(CO)_3(tmphen)^+$ and $Re(CO)_3(NO_2\text{-phen})^+$ are similar in shape and volume.

The number of quenching sites within the critical radius calculated above can be compared from the ones than can be obtained from the distances distribution of Figure 7. In polymers **V**−**VII**, the total number of quenching sites is ≈20, 50, and 100, respectively. Multiplying these numbers by the probability of ∼0.075 gives $N \approx 1.5$; 4 and 7.5 respectively.

Regarding the energy transfer process which quenches progressively the emission of the excited $Re(CO)_3(tmphen)^+$ (donor D) pendants with the increasing number of $Re(CO)_3(NO_2\text{-phen})^+$ (acceptor A) pendants in polymers **V**−**VII**, the crucial point is that when passing from polymer **V**−**VII** the probability of a donor D to be in the vicinity of an acceptor A increases. D pendants situated at distances ∼7 Å of an acceptor pendant A will be quenched instantly with k_T values around $13/\tau_D$, as d(Re−Re) = 7 Å < R_F (∼10.7 Å). D pendants situated at distances ∼20 Å (the mean distance) will be quenched with k_T values of only $0.02/\tau_D$ and will contribute less to the quenching. However, the number of acceptors at distances ∼20 Å is 3 times higher than those at distances ∼7 Å. The efficiency of energy transfer between D and A in polymers **V**−**VII** can be calculated according to

$$E_T^j = 1 - \frac{\phi_D^j}{\phi_{mb}^j} \tag{5}$$

where E_T^j represents the energy transfer efficiency in polymer j [j = **V**, **VI**, and **VII**], φ_D^j represents emission quantum yields for polymers **V**, **VI**, and **VII** and ϕ_{mb}^j are the emission quantum yields of the molar blends 90% **III** + 10% **IV**, 75% **III** + 25% **IV**, and 50% **III** + 50% **IV**, respectively. The experimental E_T^j values for polymers **V**, **VI**, and **VII** are 0.58, 0.85, and 0.94 respectively (Table 1).

Taking the E_T^j calculated above for polymers **V**−**VII**, mean values for the energy transfer rate constant between $MLCT_{Re\rightarrow tmphen}$ and $MLCT_{Re\rightarrow NO_2\text{-phen}}$ can be calculated in these polymers with the aid of eq 6:

$$\overline{k_{ET}} = \frac{1}{\tau_D}\left(\frac{E_T^j}{1 - E_T^j}\right) \tag{6}$$

The values of $\bar{k}_{ET}$ obtained for polymers **V**, **VI**, and **VII** are 2.7×10^5, 1.1×10^6, and 3.1×10^6 s^{-1}, respectively. It should be noted that those $\bar{k}_{ET}$ values are only average contributions in the polymers. In fact, in evaluating k_{ET}, it has to be assumed that the quenching of the donor D is brought about by interactions with neighboring regions of the polymer containing the acceptor molecules A. The influence of these interactions depends on the distance between D and A. Then the quenching rate for the ith donor D_i is the sum over the distance dependent interactions with j quenching sites and $\bar{k}_{ET}$ represents a mean value over all possible $k_{ET}(D_i)$:

$$k_{ET}(D_i) = \frac{1}{\tau_D}\sum_j (R_F/R(D_i,j))^6 \quad (7)$$

Using E_T^j values for polymers **V**−**VII** mean interchromophore distances can be calculated according to eq 8:

$$\bar{R} = R_F\left(\frac{1}{E_T^j} - 1\right)^{1/6} \quad (8)$$

The values of $\bar{R}$ obtained for polymers **V**, **VI**, and **VII** are 10.1, 8.0, and 6.7 Å, respectively. These $\bar{R}$ values can be compared with the D−A distances from Figure 7. For polymer **V**, a $\bar{R} = 10.1$ Å is slightly below the R_F but is 3 Å greater than the close neighbors distance (∼7 Å). $\bar{R} = 8.0$ Å for polymer **VI** implies that, on the average, donors D and acceptors A are only 1 Å apart from the close neighbors distance. In polymer **VII**, however, the mean distance between chromophores is nearly that of the close neighbors and the efficiency of energy transfer between D and A is quite high.

Flash photolysis experiments ($\lambda_{exc} = 351$ nm) on polymers **III**, **V**, **VI**, and **VII** demonstrated (Figure 4) that the $\Delta A_{t=0}$ values decrease from **III** to **VII** even when $\Delta A_{t=0}$ values are corrected for the decrease in n (i.e., from ∼200 in polymer **III** to ∼100 in polymer **VII**). For instance: $\Delta A_{t=0}$(**III**)/$\Delta A_{t=0}$(**V**) = 1.7; $\Delta A_{t=0}$(**III**)/$\Delta A_{t=0}$(**VI**) = 3.4; $\Delta A_{t=0}$(**III**)/$\Delta A_{t=0}$(**VII**) = 5.2 while $n_{(III)}/n_{(V)}$, $n_{(III)}/n_{(VI)}$ and $n_{(III)}/n_{(VII)}$ are 1.1, 1.3, and 2, respectively. $\Delta A_{t=0}$ may be considered proportional to the photogenerated concentration of the MLCT excited states in flash fotolysis experiments on polymers **III**, **V**, **VI**, and **VII**. This comparison suggests that the luminescence quenching occurs within the laser pulse lifetime (∼25 ns) when excited $Re(CO)_3(tmphen)^+$ pendants are situated at distances below R_F (∼10.7 Å) from a $Re(CO)_3(NO_2\text{-phen})^+$ acceptor and a manifestation of this "instant" quenching is the decrease of the $\Delta A_{t=0}$ values when comparing the polymers **III**−**VII** in a higher extent than $n_{(III)}/n_{(V)}$, $n_{(III)}/n_{(VI)}$ and $n_{(III)}/n_{(VII)}$. $Re(CO)_3(tmphen)^+$ excited pendants situated at distances > R_F from the acceptors $Re(CO)_3(NO_2\text{-phen})^+$ will be quenched with rate constants $k_{ET}(D_i)$ and will be observed decaying at times longer than the laser lifetime. The overall decay of all $Re(CO)_3(tmphen)^+$ excited pendants situated at distances $> R_F$ with all possible $k_{ET}(D_i)$ values will manifest in a luminescence decay according to eq 2.

The transient spectra of the polymers **III**, **V**, **VI**, and **VII** (Figure 4) decayed biexponentially over a period of several microseconds. Even the decay of the transient of polymer **III** cannot be fitted to a single exponential. However, the luminescence decay of polymer **III** after excitation with a N_2 laser ($\lambda_{exc} = 337$ nm) is monoexponential. Flash photolysis experiments were performed using an excimer laser ($\lambda_{exc} =$ 351 nm) while flash fluorescence experiments ($\lambda_{exc} = 337$ nm) were performed using a N_2 laser. The energy/pulse from the excimer laser is ∼15 times higher than that in flash fluorescence experiments. As a consequence, much higher concentrations of MLCT are produced in flash photolysis experiments than in flash fluorescent ones. We have previously observed marked differences (i.e., biexponenetial in contrast to monoexponential decays) when the MLCT excited-state of the polymer $[(vpy)_2\text{-}vpyRe(CO)_3(2,2'\text{-bipyridine})^+]_{n\sim200}$ were generated in either high or low concentrations.[9] Such differences were related to MLCT annihilation processes in addition to the first order decay due to the presence of excited chromophores in close proximity in the polymer.[1,9] The existence of Re^I chromophores in diverse environments was shown by the intrinsic kinetics of the luminescence, the decay kinetics of the MLCT excited states observed by time-resolved-absorption spectroscopy, and the quenching of the luminescence by various quenchers, with related mixed polymers $\{(vpy\text{-}[Re(CO)_3(2,2'\text{-bpy})])_m(vpy\text{-}Re(CO)_3(phen)])_n(vpy)_p\text{-}(CF_3SO_3)_{m+n}\}$, $m = 131$, $n = 131$ or $m = 200$, $n = 150$, and $m + n + p = 600$. These experimental observations account for the presence of medium-destabilized charge-transfer excited states, in some chromophores within a strand of polymer.[28] Therefore, as the MLCT decay in polymers **V**−**VII** is much more complex in flash photolysis experiments than in flash fluorescent ones due to the higher concentrations of excited chromophores generated in the former experiments, the absorbance decay of the generated transients was fitted to a biexponential decay rather than that of eq 2 used to fit luminescence profiles decays. As it can be observed from Table 1, the two lifetimes τ_{fast} and τ_{slow} decrease from polymers **V** to **VII** in accordance with the increase in parameter a obtained from luminescence decay profiles. However, we are aware that the transient decay probably is not a truly biexponential and the two lifetimes may be corresponding to a random distribution of decay times which are approximately fitted to a sum of two exponentials and the two lifetimes may represent average contributions from excited chromophores in different environments.

Conclusions

We have prepared inorganic polymers derived from the poly-4-vinylpyridine backbone with attached $Re(CO)_3(tmphen)^+$ and $Re(CO)_3(NO_2\text{-phen})^+$ chromophores with a general formula of $\{[(vpy)_2\text{-}vpyRe(CO)_3(tmphen)^+]\}_n\{[(vpy)_2vpyRe(CO)_3(NO_2\text{-phen})^+]\}_m$. The ratio n/m was varied from 9 to 1 maintaining $n + m \sim 200$. Multiple morphologies of aggregates from these Re^I polymers were obtained from TEM images of their solvent-cast films by using acetonitrile and dichloromethane as solvents. Regarding the polymers photophysical properties, as the ratio n/m decreases, the substitution of pendants $Re(CO)_3(tmphen)^+$ by pendants $Re(CO)_3(NO_2\text{-phen})^+$ in the poly-4-vinylpyridine backbone produces a decrease in ϕ_{em} that is in proportion to the number of $Re(CO)_3(NO_2\text{-phen})^+$ pendants relative to that of $Re(CO)_3(tmphen)^+$ pendants due to an energy transfer process that involves the excited states $MLCT_{Re\rightarrow tmphen}$ and $MLCT_{Re\rightarrow NO_2\text{-phen}}$. Luminescence lifetimes and emission quantum yields results were discussed in terms of FRET theories applied to polymers. A good comparison was observed between the number of quenching sites within the Förster's critical radius obtained from luminescence lifetimes and from the results of a molecular modeling calculation on the Re^I polymers.

Acknowledgment. Work supported in part by ANPCyT Grant No. PICT 06-12610, CONICET-PIPs 2470/00 and 6301/05, Universidad Nacional de La Plata, and CICPBA. G.F. acknowledges support from the Office of Basic Energy Sciences of the U.S. Department of Energy. L.L.B.B. acknowledge support from CONICET. The authors wish to thank Mr. Fernando Amarilla for performing the viscosity measurements. This is contribution No. NDRL-4747 from the Notre Dame Radiation Laboratory.

Supporting Information Available: Figures showing the UV−vis and IR spectra of polymers **III**, **IV**, **V**, **VI**, and **VII** and emission spectra of polymers **III**, **V**, **VI**, and **VII** and a table containing all the Re−Re distances obtained from molecular modeling calculations and used in the preparation of Figure 7. This material is available free of charge via the Internet at http://pubs.acs.org.

References and Notes

(1) Wolcan, E.; Ferraudi, G. J. *Phys. Chem. A* **2000**, *104*, 9281.
(2) Jones, W. E.; Hermans, L., Jr.; Jiang, B. In *Multimetallic and Macromolecular Inorganic Photochemistry*; Ramamurthy, V., Schanze, K. S., Eds.; Marcel Dekker Inc.: New York, 1999; Vol *4*. Chapter 1.
(3) Ogawa, M. Y. In *Multimetallic and Macromolecular Inorganic Photochemistry*; Ramamurthy, V., Schanze, K. S., Eds.; Marcel Dekker Inc.: New York, 1999; Vol *4*, Chapter 3.
(4) Stufkens, D. J.; Vlček, A., Jr *Coord. Chem. Rev.* **1998**, *177*, 127, and references therein.
(5) Smith, G. D.; Maxwell, K. A.; DeSimone, J. M.; Meyer, T. J.; Palmer, R. A. *Inorg. Chem.* **2000**, *39*, 893.
(6) Petersen, J. D. In *Supramolecular Photochemistry*; Balzani, V., Ed.; Reidel: Dordrecht, The Netherlands, 1987; p 135.
(7) Balzani, V.; Scandola, F. In *Supramolecular Photochemistry*; Ellis Harwood: Chichester, U.K., 1991; p 355.
(8) Kaneko, M.; Tsuchida, E. *J. Polym. Sci.* **1981**, *16*, 397.
(9) Wolcan, E.; Feliz, M. R. *Photochem. Photobiol. Sci.* **2003**, *2*, 412.
(10) Wolcan, E.; Ferraudi, G.; Feliz, M. R.; Gomez, R. V.; Mickelsons, L. *Supramol. Chem.* **2003**, *15*, 143.
(11) Feliz, M. R.; Ferraudi, G. *Inorg. Chem.* **2004**, *43*, 1551.
(12) Wolcan, E.; Alessandrini, J. L.; Feliz, M. R. *J. Phys. Chem. B* **2005**, *109*, 22890.
(13) Forster, T. *Discuss. Faraday Soc.* **1959**, *27*, 7.
(14) Herz, L. M.; Silva, C.; Grimsdale, A. C.; Müllen, K.; Phillips, R. T. *Phys. Rev B* **2004**, *70*, 165207.
(15) Srinivas, G.; Bagchi, B. *J. Chem. Phys.* **2002**, *116*, 837.
(16) Rolinski, O. J.; Mathivanan, C.; Macnaught, G.; Birch, D. J. S. *Biosensors Bioelectron.* **2004**, *20*, 424.
(17) Tcherkasskaya, O.; Klushin, L.; Gronenborn, M. *Biophys. J.* **2002**, *82*, 988.
(18) Selvin, P. R. *Nat. Struct. Biol.* **2000**, *7*, 730.
(19) Salthammer, T.; Dreeskamp, H.; Birch, D. J. S.; Imhof, R. E. *J. Photochem. Photobiol. A: Chem.* **1990**, *55*, 53.
(20) Birch, D. J. S.; Rolinski, O. J.; Hatrick, D. *Rev. Sci. Instrum.* **1996**, *67*, 2732.
(21) Draxler, S.; Lippitsch, M. E. *Anal. Chem.* **1996**, *68*, 753.
(22) Birch, D. J. S.; Holmes, A. S.; Darbyshire, M. *Meas. Sci. Technol.* **1995**, *6*, 243.
(23) Hallam, A.; Birks, J. B. *J. Phys. B: At. Mol. Phys.* **1978**, *11*, 3273.
(24) Feliz, M. R.; Ferraudi, G. *J. Phys. Chem.* **1992**, *96*, 3059.
(25) Feliz, M. R.; Ferraudi, G.; Altmiller, H. *J. Phys. Chem.* **1992**, *96*, 257.
(26) Guerrero, J.; Piro, O. E.; Wolcan, E.; Feliz, M. R.; Ferraudi, G.; Moya, S. A. *Organometallics* **2001**, *20*, 2842.
(27) N_t is the number of molecules which survived excitation at time t, τ_D is the excited state lifetime of the donor in the absence of transfer, R_F is the Förster critical radius, and a is a parameter proportional to the density of acceptor quenching sites which can be calculated according to $a = {}^4/_3\pi^{3/2}\rho R_F{}^3$ where ρ stands for the number of quenching sites per volume. N_t relates the form of the decay curve to a certain quenching mechanism (in our case Forster's dd energy transfer) and two structural quantities, namely the density of quenching sites and the critical radius R_F. The number of quenching sites within the critical radius is given by $N = a/\sqrt{\pi}$. The Förster critical radius was calculated according to $(R_F/\mathrm{cm})^6 = 8.79 \times 10^{-25}$-$[\kappa^2\phi_D/n^4]\int[f_D(\upsilon)\varepsilon_A(\upsilon)\ \mathrm{d}\upsilon]/[\mathrm{dm}^3\ \mathrm{mol}^{-1}\ \mathrm{cm}^3\ \upsilon^4]$ where κ^2 is an orientation factor equal to ${}^2/_3$ for an isotropic angular distribution, n is the refractive index of the medium, ϕ_D is the quantum yield of the emission donor, $\varepsilon_A(\upsilon)$ is the decadic extinction coefficient of the acceptor at wavenumber υ, and $f_D(\upsilon)$ is the emission spectrum of the donor such that $\int f_D(\upsilon)\ \mathrm{d}\upsilon$ is unity.
(28) Wolcan, E.; Féliz, M. R.; Alessandrini, J. L.; Ferraudi, G. *Inorg. Chem.* **2006**, *45*, 6666.
(29) Wallace, L.; Rillema, D. P. *Inorg. Chem.* **1993**, *32*, 3836.
(30) Busby, M.; Gabrielsson, A.; Matousek, P.; Towrie, M.; Di Bilio, A. J.; Gray, H. B.; Vlček, A. *Jr. Inorg. Chem.* **2004**, *43*, 4994.
(31) Scholes, G. D. *Annu. Rev. Phys. Chem.* **2003**, *54*, 57.
(32) Wilkinson, F. In *Photoinduced Electron Transfer*; Fox, M. A. ,Chanon, M., Eds.; Elsevier: Oxford, 1988; p 208.
(33) Rhee, M. J.; Sudnick, D. R.; Arkle, V. K.; Horrocks, W. D., Jr *Biochemistry* **1981**, *20*, 3328.
(34) Snyder, A. P.; Sudnick, D. R.; Arkle, V. K.; Horrocks, W. D., Jr *Biochemistry* **1981**, *20*, 3334.
(35) Anni, M.; Manna, L.; Cingolani, R.; Valerini, D.; Cretí, A.; Lomascolo, M. *App. Phys. Lett.* **2004**, *85*, 4169.
(36) Selvin, P. R. *Annu. Rev. Biophys. Biomol. Struct.* **2002**, *31*, 275.
(37) Hemmilä, I.; Laitala, V. *J. Fluoresc.* **2005**, *15*, 529.
(38) Xiao, M.; Selvin, P. R. *Rev. Sci. Instrum.* **1999**, *70*, 3877.
(39) Selvin, P. R. *IEEE J. Selected Top. Quantum Electron.* **1996**, *2*, 1077.
(40) Selvin, P. R.; Tariq, M.; Rana, T. M.; Hearst, J. E. *J. Am. Chem. Soc.* **1994**, *116*, 6029.
(41) Huynh, M. H. V.; Dattelbaum, D. M.; Meyer, T. J. *Coord. Chem. Rev.* **2005**, *249*, 457.
(42) Turro, N. J. *Modern Molecular Photochemistry*; University Science Books: Mill Valley, CA, 1991; Chapter 9, p 296.

JP802241K